

Conduction-Electron Relaxation Time and de Haas-van Alphen Effect in Zn-Mn Alloys

B. E. PATON,* F. T. HEDGCOCK,† AND W. B. MUIR

Eaton Electronics Research Laboratory, McGill University, Montreal, Quebec, Canada

(Received 12 June 1970)

We report the observation of a weak magnetic field dependence in the collision parameter for the de Haas-van Alphen effect in the field range 3–10 kG of a Zn-Mn crystal containing 64 ppm Mn. This dependence can be adequately accounted for if the collision parameter is permitted to be a function of magnetic field as well as temperature. The field dependence of the collision parameter which results from the freeze-out of spin-flip scattering is deduced from the magnetoresistance in the same alloy.

Two of the authors¹ showed how the energy-dependent relaxation time described by Kondo² could be included in the de Haas-van Alphen (dHvA) effect and used to explain the dHvA amplitude observed at low fields in a dilute alloy of Mn in Zn.³ Recently, new experimental evidence⁴ suggests that the collision parameter (Dingle temperature) for these alloys scales logarithmically with temperature in the same manner as the electrical resistivity. Such a correlation would be expected from a solely temperature-dependent relaxation time. However, the experimental dHvA amplitudes at two different temperatures as a function of the inverse field were found to cross over at a finite field value,⁵ a property which cannot be explained by either an energy- or temperature-dependent relaxation time. In this paper we report the observation of a weak magnetic field dependence in the collision parameter for the field range 3–10 kG. It will be shown that the freezing out of the spin degree of freedom by the applied field is responsible for the observed field dependence of the collision parameter and for the crossover of the dHvA amplitudes at a finite field value.

For Zn-Mn we find the harmonic content of the dHvA oscillations is small and hence the conduction-electron differential magnetization ν is given by⁶

$$\nu = C \frac{T}{H^{1/2}} \frac{\sin(2\pi F/H - \phi)}{\sinh(2\pi^2 kT/\beta^* H)} \exp\left(-\frac{2\pi^2 kX}{\beta^* H}\right), \quad (1)$$

where C is a constant independent of T and H , $F = \hbar A/2\pi e$, A is the extremal cross section of the Fermi surface perpendicular to H , $\beta^* = eh/m^*c$, m^* is the cyclotron effective mass, ϕ is the dHvA phase factor, and the collision parameter X is related to the relaxation time τ by

$$X = \hbar/2\pi k\tau. \quad (2)$$

The amplitude of the oscillations $|\nu|$ can be expressed as

$$\alpha = (\beta^*/2\pi^2 k) \ln C - XH^{-1},$$

where

$$\alpha = \frac{\beta^*}{2\pi^2 k} \ln \left[\frac{|\nu| H^{1/2}}{T} \sinh\left(\frac{2\pi^2 kT}{\beta^* H}\right) \right]. \quad (3)$$

For normal scattering mechanisms, a graph of α against H^{-1} gives a temperature-independent straight line having slope X .

In the present paper, the field modulation technique described by Goldstein *et al.*⁶ has been used to measure the “needle” orbit P_1 and two orbits on the second-zone hole “monster” surface P_2 and P_3 . The measurements were made with a modulation frequency of 3 kHz, at magnetic fields between 3 and 50 kG and temperatures from 1.1 to 4.2°K. The modulation amplitude was fixed over the range of fields used and the differential magnetization was deduced after scaling by the appropriate Bessel function and correcting for the variation of skin depth with field.⁶ The alloy sample used was cut from the Zn 64 at. ppm Mn crystal previously used in resistivity studies⁷ which displayed the characteristic $\ln T$ term in the resistivity associated with the Kondo effect. The crystal orientation for the dHvA studies was at an angle $\theta = 78^\circ$ to the c axis in the (010) symmetry plane, where the effect of magnetic breakdown⁸ in the needle orbit is small (0.3%) in the field region $H < 10$ kG.

The effect of alloying with 64 at. ppm Mn on the Fermi surface of zinc is extremely small and no change in the period or effective-mass ratio was observed in the alloy. The dHvA amplitude of the needle orbit is shown in Fig. 1 and the temperature dependence of the collision parameter³ as shown in Fig. 2 is immediately evident. A weak field dependence which increases with decreasing temperature is also observed in the field region $3 \text{ kG} < H < 10$ kG. No field dependence due to magnetic scattering was observed in the previous investigations^{3–5} in the field region $H < 3$ kG. The crossover of two different temperature curves noted by Holt and Meyers⁵ is also present in our data. The signal-to-noise ratio at low fields and the beating of the periods P_2 with P_1 at high fields limited reliable measurements to the field range $3 \text{ kG} < H < 12$ kG and temperatures below 3.6°K. No field or temperature dependence was observed in the larger orbits on the second-zone monster surface. This agrees with similar null results by Holt and Meyers⁵ for the orbit P_2 and the lens orbit P_{13} .

The magnetic scattering was introduced into the

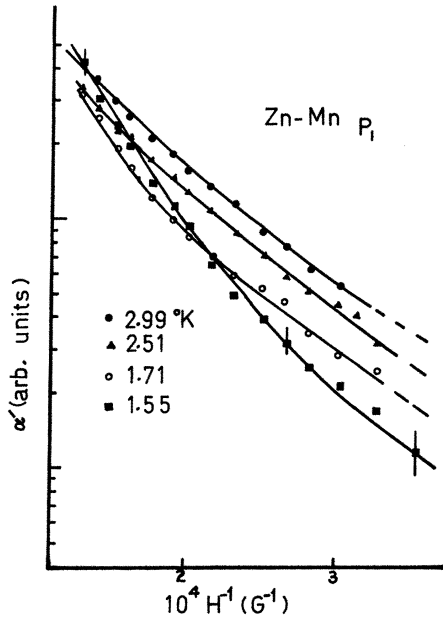


FIG. 1. Field dependence of the dHvA amplitude of the needle orbit P_1 in a Zn 64 ppm Mn crystal. The value of α is related to the ordinate α' by $\alpha = (\beta^*/2\pi^2k) \ln \alpha'$. The value of $\beta^*/2\pi^2k$ is 2.24×10^{-4} Oe/ $^\circ$ K.

expression for the collision parameter using Brailsford's relationship⁹

$$(x/x_p) = f, \tag{4}$$

where f is a constant which will be taken as 1 for convenience¹⁰ and $x_p(H, T)$ is the effective resistivity collision parameter due to the spin component of the

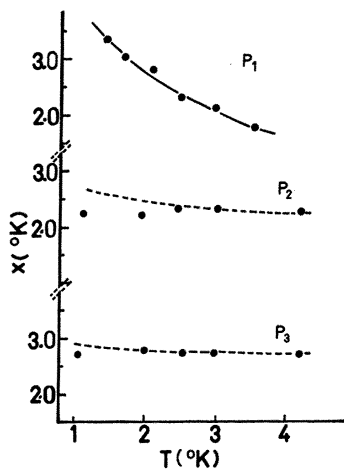


FIG. 2. Temperature dependence of the collision parameters for the orbits P_1 , P_2 , and P_3 in the Zn-Mn crystal. The solid line in P_1 is the calculated collision parameters from Eq. (8); see text. The dashed lines for P_2 and P_3 are the type of variation that would be expected if J_{s-d} for the monster orbits were the same as that for the needle orbit.

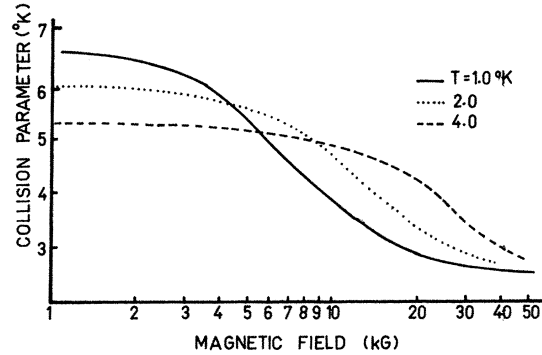


FIG. 3. Field dependence of the collision parameter $X(H, T)$ for various temperatures calculated using Eq. (7).

resistivity $\rho_m(H, T)$ as follows:

$$x_p(H, T) = ne^2\hbar\rho_m(H, T)/2\pi km, \tag{5}$$

where n is the number of electrons/cm³ and m is the free-electron mass.

The field dependence in the resistivity arises from the freezing out of the spin-flip scattering as calculated to second order by Yosida¹¹ and later carried to third order¹² to include the Kondo term. The influence of the applied field in the temperature region $T > T_k$ is felt mainly in the second-order term ρ_m which scales as the square of the magnetization.¹³ Since $T > T_k$ for Zn-Mn at helium temperatures,¹⁴ the local moment can be considered as a free spin¹⁵ and the magnetization approximated by $M = Ng\mu_0 SB_s(y)$, where $B_s(y)$ is the Brillouin function and $y = gS\mu_0 H/kT$. Magnetoresistance results¹⁶ on dilute polycrystalline alloys of Zn-Mn indicated that the resistance in a finite field can be described by¹⁷

$$\rho_m(H, T) = c\rho_A + c\rho_m[1 + D(0)J \ln T] \times \{1 - [\gamma S^2/S(S+1)]B_s^2(y)\}, \tag{6}$$

where $c\rho_A$ is the potential scattering term,

$$c\rho_m = 3c\pi m J^2 S(S+1)/2ne^2\hbar E_0$$

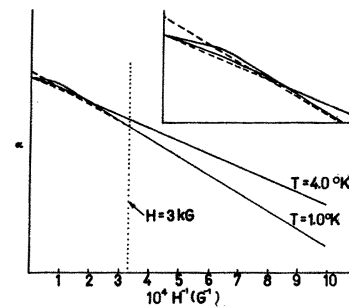


FIG. 4. Field dependence of the dHvA amplitude calculated using Eq. (10). The low-field extrapolation to infinite fields is shown as the dashed line.

is the magnetic scattering term, S is the impurity spin (equal to $\frac{3}{2}$ for Zn-Mn¹⁸), $D(0)$ is the one-electron density of states per spin for the host, J is the s - d exchange constant, and the parameter γ is well approximated by $1+1/g^2S(S+1)$. Using Eq. (6) the collision parameter determined from Eq. (5) becomes

$$X(H, T) = X_0 + X_K(T) \left(1 - \frac{\gamma S^2}{S(S+1)} B_s^2(y) \right), \quad (7)$$

where

$$X_K(T) = (\hbar/2\pi k) [(ne^2/m)c\rho_m][1 + D(0)J \ln T], \quad (8)$$

$$X_0 = ne^2\hbar c\rho_A/2\pi km, \quad \text{which is a constant.} \quad (9)$$

It is interesting to point out that in the absence of the field-dependent term, i.e., $B(y)=0$, the above expression is identical to the expression derived⁴ from a solely temperature-dependent relaxation time. Figure 3 shows $X(H, T)$ as a function of H for various temperatures as calculated from Eq. (7). In the high-field region where the Brillouin function saturates, the collision parameter becomes solely temperature dependent, whereas, in the low-field region where the Brillouin function scales as (H/T) , serious discrepancies with a solely temperature-dependent collision parameter are expected.

When the collision parameter, Eq. (7), is included in Eq. (3), the dHvA amplitude function α can be written as

$$\alpha = \xi_0 - \frac{X_0 + X_K(T)}{H} + \frac{X_K(T)}{H} \left(\frac{\gamma S^2}{S(S+1)} B_s^2(y) \right). \quad (10)$$

Figure 4 shows α as a function of H calculated from Eq. (10) using $X(0, T)$ obtained from the low-field results³ where the field-dependent scattering is small.¹⁹ The following features are evident:

(i) The existence of a collision parameter which is temperature dependent.

(ii) An intersection for two different temperature curves occurs at a finite value of $1/H$. The temperature dependence of the infinite-field intercept $\alpha_\infty(T)$ is the result of the low-field extrapolation to infinite field shown in Fig. 4 as a dashed line. These values of $\alpha_\infty(T)$ are compared to the experimental values of Ref. 3 in Table I.

(iii) The curves for different temperatures converge to the same value at $1/H=0$, as expected from the Lifshitz-Kosevich theory.²⁰

(iv) A weak magnetic field dependence exists in the field range 3–30 kG, the magnitude of which increases

TABLE I. Comparison of the experimental results of Ref. 3 for the collision parameter and infinite-field intercept α_∞ with the values of these parameters calculated in the present paper for the P_1 orbit.

Temperature (°K)	Collision parameter (°K)		Infinite-field intercept (10 ⁻³ °K/Oe)	
	Expt	Calc	Expt	Calc
1.7	6.1±0.2	6.22	3.54±0.04	3.69
2.6	5.7±0.2	5.72	3.44±0.04	3.42
4.2	5.2±0.2	5.20	3.34±0.04	3.38

with decreasing temperature. The magnetic field dependence is negligible for fields less than 3 kG.

Since the low-field amplitude of the P_1 orbit oscillations could not be accurately measured in the present experiments, it was impossible to directly determine $X(0, T)$. A first approximation to $X(0, T)$ was obtained from a best straight-line fit to α as a function of H^{-1} [Eq. (3), Fig. 1]. This with Eqs. (7) and (8) allowed X_0 and $ne^2\hbar c\rho_m/2\pi km$ to be estimated.¹⁹ The quantity $D(0)J$ was determined from the collision parameter measured at 3.6°K, where little or no curvature in α as a function of H^{-1} was observed. Using these parameters and Eqs. (8) and (10), α was calculated as a function of H^{-1} , ξ_0 being chosen to obtain a fit of the calculated and experimental values of α at $H^{-1}=3 \times 10^{-4} \text{ G}^{-1}$. The results of this calculation are shown as the solid lines in Fig. 1. The value of $X_0 + X_K(T)$ calculated from Eq. (8) for the P_1 orbits is shown as the solid line in Fig. 2. As seen in Figs. 1 and 2, good agreement between the experimental and theoretical values of the amplitude and the collision parameter is obtained.

For the P_2 and P_3 orbits α is a linear function of H^{-1} and the values of X are as shown by the points in Fig. 2. The solid curves are scaled from the (H/T) dependence of the collision parameter for the P_1 orbits using Eq. (7) and fitted to the values of X at a temperature of 4.2°K. Although the estimated magnitude of the effect for these orbits is greater than the experimental error, no temperature dependence was observed. The simplest and most immediate suggestion for the nonobservation of the effect would be a difference in the value for J_{s-d} between the needle and monster surfaces.

The authors would like to acknowledge useful discussions with Dr. I. M. Templeton, Dr. P. T. Coleridge, Dr. D. W. J. Geldart, Dr. M. J. Zuckermann, Dr. A. Myers, and Dr. J. Vanderkooy. One of us (B.E.P.) received financial assistance through a J. W. McConnell Memorial Fellowship.

* Research completed in partial fulfillment of the Ph.D. degree at McGill University.

† Research supported by Grant No. A2329 from the National Research Council of Canada.

¹ B. E. Paton and W. B. Muir, Phys. Rev. Letters **20**, 732 (1968).

² J. Kondo, Progr. Theoret. Phys. (Kyoto) **32**, 27 (1964).

³ F. T. Hedgcock and W. B. Muir, Phys. Rev. **129**, 2045 (1963).

⁴ H. Nagasawa, Solid State Commun. **7**, 259 (1969).

⁵ G. Holt and A. Myers, Physik Kondensierten Materie **9**, 23 (1969).

⁶ A. Goldstein, S. J. Williamson, and S. Foner, *Rev. Sci. Instr.* **36**, 1356 (1965); L. F. Chollet and I. M. Templeton, *Phys. Rev.* **170**, 656 (1968).

⁷ M. J. Press and F. T. Hedgcock, *Phys. Rev. Letters* **23**, 167 (1969).

⁸ R. J. Higgins and J. A. Marcus, *Phys. Rev.* **161**, 589 (1967).

⁹ A. D. Brailsford, *Phys.* **149**, 456 (1966).

¹⁰ This can be utilized since the constant f can be determined by plotting the collision parameter as a function of the experimental resistivity. With a suitable assumption for the size of the normal potential scattering term $c\rho_A$ (see Ref. 2), f is estimated as approximately 1.1.

¹¹ K. Yosida, *Phys. Rev.* **106**, 893 (1957).

¹² M. T. Béal-Monod and R. A. Weiner, *Phys. Rev.* **170**, 552 (1968).

¹³ P. Monod, *Phys. Rev. Letters* **19**, 1113 (1967); F. T. Hedg-

cock, W. B. Muir, T. W. Raudorf, and R. Szmidt, *ibid.* **20**, 457 (1968).

¹⁴ $T_K \approx 0.2$; see R. S. Newrock, B. Serin, and G. Boato, *Bull. Am. Phys. Soc.* **14**, 371 (1969).

¹⁵ D. J. Scalapino, *Phys. Rev. Letters* **16**, 937 (1966).

¹⁶ B. E. Paton and M. J. Press, in *Proceedings of the Canadian Metal Physics Conference, 1969* (unpublished).

¹⁷ This expression can be obtained from the results of Ref. 12 by including the Brillouin function $B_s(y)$ in the expression for the magnetization M .

¹⁸ E. W. Collings, F. T. Hedgcock, and Y. Muto, *Phys. Rev.* **134**, A1521 (1964).

¹⁹ Using an approximation equivalent to Kondo's (Ref. 2), X_0 is assumed equal to $n^2\hbar c\rho_m/2\pi km$ and to $\frac{1}{2}X(0, 1^\circ)$.

²⁰ I. A. Lifshitz and A. M. Kosevich, *Zh. Eksperim. i Teor. Fiz.* **29**, 730 (1955) [*Soviet Phys. JETP* **2**, 636 (1956)].

High-Temperature Wavelength-Dependent Properties of a Heisenberg Paramagnet*

M. F. COLLINS

Physics Department, McMaster University, Hamilton, Ontario, Canada

(Received 17 July 1970)

The first four terms of the high-temperature expansion of the wavelength-dependent susceptibility $\chi(\mathbf{k})$ and the spin correlation function $S(\mathbf{k})$ are calculated. Nearest-neighbor exchange interactions are assumed with general spin values and a Bravais lattice. From these results the first four terms in the high-temperature expansion of the effective range of the spin correlation are obtained for both ferromagnets and antiferromagnets. The terms are slightly different according to whether the range is defined from $\chi(\mathbf{k})$ or from $S(\mathbf{k})$, though they become identical limitingly close to the critical ordering temperature. The calculated properties can all be measured by current neutron scattering techniques.

I. INTRODUCTION

In a recent paper Fisher and Burford¹ have given a comprehensive study of the wavelength-dependent properties of the Ising model. It would be desirable if we could get similar insight into the Heisenberg model with general spin value S , since this corresponds to a case more commonly occurring in nature. The purpose of this paper is to investigate the high-temperature expansion of the wavelength-dependent properties of this Heisenberg model.

An immediate extra complication arises for the Heisenberg Hamiltonian over the Ising case because there are two distinct wavelength-dependent properties of interest. These are $\chi(\mathbf{k})$, the susceptibility, and $S(\mathbf{k})$, the spatial Fourier transform of the two-spin correlation function, where \mathbf{k} is a general vector in reciprocal space. For the Ising model these two quantities are the same, to within a constant factor; the differences arise essentially because the Heisenberg Hamiltonian does not commute with S^z on any particular atom while the Ising Hamiltonian does. For the Heisenberg Hamiltonian the two quantities only become the same at $\mathbf{k}=0$ or in the limit as S tends to infinity (the "classical model").

This paper deals with the expansion of both $\chi(\mathbf{k})$ and $S(\mathbf{k})$ at high temperatures. For the special cases of $\chi(0)$ and $\chi(\boldsymbol{\tau})$, where $\boldsymbol{\tau}$ is an antiferromagnetic

reciprocal-lattice vector of a loose-packed material, Rushbrooke and Wood^{2,3} have given the expansions to six terms. This involved a laborious calculation and, seeing that the analogous calculations at general wave vectors are even more laborious, this work only goes as far as the fourth term for a general Bravais lattice of spins.

Given the functions $\chi(\mathbf{k})$ and $S(\mathbf{k})$, an expansion can be made about the point $\mathbf{k}=0$ to give

$$\chi(\mathbf{k}) = \chi(0)[1 - \xi_x^2 k^2 + O(k^4)] \quad (1)$$

and

$$S(\mathbf{k}) = S(0)[1 - \xi_s^2 k^2 + O(k^4)]. \quad (2)$$

The quantity ξ as defined by the above equations is known as the effective range of spin correlation.¹ For the Heisenberg Hamiltonian there are two such effective ranges ξ_s and ξ_x defined from the functions $S(\mathbf{k})$ and $\chi(\mathbf{k})$, respectively. It can be shown that the effective ranges become equal in the limit as the temperature approaches the critical ordering temperature from above so that the parameters have the same critical exponent ν_1 .

The quantities $S(\mathbf{k})$, $\chi(\mathbf{k})$, ξ_x , and ξ_s which are calculated in this paper are all observable quantitatively by current neutron scattering techniques. The physical principles involved in such experiments have been reviewed recently by Marshall and Lowde⁴ and